*Progress In Electromagnetics Research, PIER 73, 49–59, 2007*

# NEAR-FIELD TO FAR-FIELD TRANSFORMATION WITH PLANAR SPIRAL SCANNING

**S. Costanzo and G. Di Massa**

Dipartimento di Elettronica
Informatica e Sistemistica
Universitá della Calabria
87036 Rende (CS), Italy

**Abstract**—A transformation procedure directly computing the antenna far-field pattern from near-field samples acquired on a planar spiral is proposed in this paper. The convolution property of the radiation integral is exploited to efficiently perform the evaluation by taking advantages of the Fast Fourier Transform, without the need of any intermediate interpolation process. Validations on circular arrays of elementary dipoles are presented to show the effectiveness of the method.

## 1. INTRODUCTION

Measuring techniques in the radiating near-field are established as compact and controlled environments to perform accurate antenna test and diagnostics. They require a processing of the probed near-field distribution to recover the corresponding far-field pattern, with a variety of existing transformation techniques based on modal expansions and equivalent source reconstruction, or employing trained neural networks [1]. Standard near-field setup are based on planar, cylindrical and spherical geometries, but improved scanning configurations, in terms of complexity and cost, have been introduced. In the framework of planar near-field measurements, a strong improvement with respect to scanner compactness is given by the bi-polar configuration [2], based on exclusive rotational motions of the Antenna Under Test (AUT) and the measuring probe. Near-field data are collected at the intersections between concentric rings and radial arcs, by imposing a full revolution of the AUT, followed by an incremental rotation of the probe arm. A further improvement of

the bi-polar configuration has been recently achieved by imposing a simultaneous and continuous motion of the AUT and the measuring probe, so reducing the acquisition time as well as the overall system complexity. This measurement strategy results in a sampling arrangement on a planar spiral [3], which however strongly complicates the near-field to far-field transformation process, as a conversion to a rectangular format is needed to take advantage of the Fast Fourier Transform (FFT) algorithm. An Optimal Sampling Interpolation (OSI) technique [4] is then applied [3] to express the radiating field in a cardinal series form by employing appropriate sampling functions. An approximate interpolation formula is also adopted [3] to map the non-uniform behavior of spiral samples in the radial coordinate into a sequence of uniformly spaced data. In order to avoid the near-field oversampling inherent to the spiral sampling arrangement, a fast and accurate interpolation algorithm is proposed in [5, 6] to reconstruct the radiated electromagnetic field on a rotational surface from the knowledge of a non redundant number of its samples on a spiral wrapping the scanning surface. In this paper, a fast data processing algorithm is proposed to compute the AUT far-field directly from near-field samples acquired on the planar spiral. The convolution property of the radiation integral is exploited to develop an efficient procedure computing the far-field pattern in terms of FFT algorithm. This avoids the application of intermediate interpolations usually adopted in literature to enable the use of planar near-field to far-field transformation. Numerical simulations on circular arrays of Huyghens sources are discussed to validate the proposed technique.

## 2. NEAR-FIELD SAMPLING ON PLANAR SPIRAL

The planar spiral geometry is obtained by imposing a simultaneous rotation of the AUT and the probe arm in terms of angles $\alpha'$ and $\beta'$, respectively (Fig. 1). This gives a samples distribution on radial arcs at points $P(s', \alpha')$ (Fig. 2), where $s'$ is a surrogate for the radial coordinate $\rho'$, defined as [3]:

$$s' = \frac{\rho'}{d} \tag{1}$$

The parameter $d$ in relation (1) gives the distance between the AUT and the near-field measuring plane (fig.1), while $\alpha'$ is the angle describing the AUT rotation, which is related to the azimuthal coordinate $\phi'$ by the equation [2]:

$$\alpha' = \phi' + \frac{\beta'}{2} \tag{2}$$

$\beta'$ being the probe arm rotation angle.

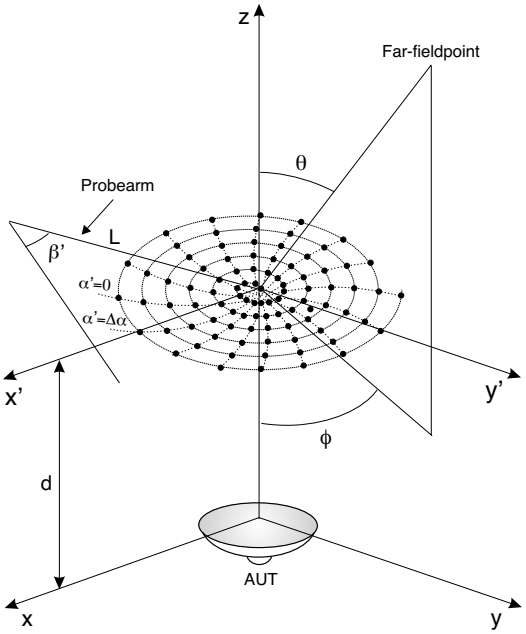


**Figure 1.** Planar spiral scanning geometry.

The archimedean spiral scanning is mathematically described by the equation:

$$\rho' = a\alpha' + 2\pi a\gamma, \quad a > 0, \quad \gamma = 0, 1, 2, ... \tag{3}$$

which identifies all points lying on the radial arc associated to a specific value of the azimuthal angle $\alpha'$ (Fig. 2).

The radial spacing between two adjacent points on the same arc is derived from (3) as:

$$\Delta\rho = 2\pi a \tag{4}$$

It must be coherent with the sample spacing needed for the plane-polar geometry, that is:

$$\Delta\rho = \frac{\lambda}{2} \tag{5}$$

So, the correct value for the parameter $a$ into expression (3) is derived from sampling considerations, by equating relations (4) and (5) to

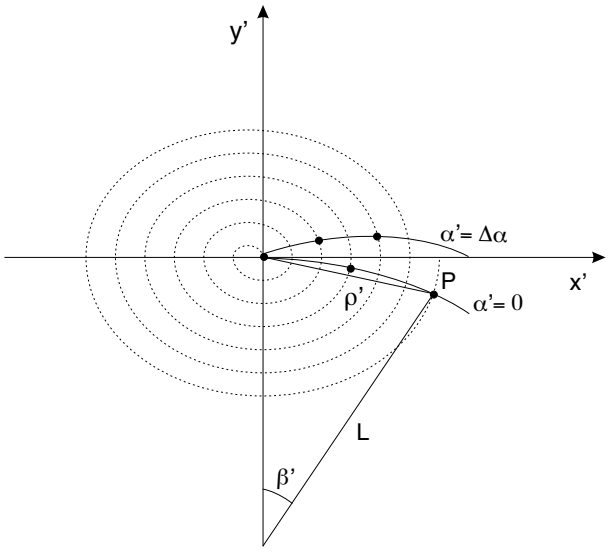


**Figure 2.** Sampling arrangement on planar spiral.

obtain:

$$a = \frac{\lambda}{4\pi} \tag{6}$$

## 3. FAR-FIELD COMPUTATION FROM NEAR-FIELD ON PLANAR SPIRAL

Let us consider a near-field data set collected on a polar scan plane having radius $\rho_{max}$. A radiation-type integral for the equivalent aperture current on the acquisition plane can be derived as [7]:

$$T(\theta,\phi) = \int_0^{\rho_{max}} \int_0^{2\pi} q(\rho',\phi') \cdot e^{jk\rho' sin\theta cos(\phi-\phi')} \rho' d\rho' d\phi' \tag{7}$$

where the scalar form is considered, for the sake of simplicity.

Under the assumption of a omnidirectional probe, the left hand side of equation (7) gives the far-field at coordinates ($\theta$,$\phi$) (Fig. 1), while the term $q(\rho',\phi')$ represents the near-field distribution on the measurement plane $x'$-$y'$ (Fig. 1), $k$ being the free-space propagation constant.

In the presence of a near-field spiral trajectory with maximum radial extension $\rho_{max}$, the coordinate transformations (1), (2) from polar

variables $(\rho', \phi')$ to spiral variables $(s', \alpha')$ modifies the radiation integral (7) as follows:

$$T(\theta,\phi) = \int_0^{\frac{\rho_{max}}{d}} \int_{\frac{\beta'}{2}}^{\frac{\beta'}{2}+2\pi} q(s',\alpha') \cdot e^{jkds'sin\theta cos(\phi-\alpha'+\frac{\beta'}{2})} d^2 s' ds' d\alpha' \quad (8)$$

A compact form of equation (8) can be easily derived as:

$$T(\theta,\phi) = \int_0^{\frac{\rho_{max}}{d}} \int_{\frac{\beta'}{2}}^{\frac{\beta'}{2}+2\pi} q_1(s',\alpha') \cdot r(\theta,\phi,s',\alpha') ds' d\alpha' \quad (9)$$

where the following definitions are adopted:

$$q_1(s',\alpha') = s' d^2 q(s',\alpha') \quad (10)$$

$$r(\theta,\phi,s',\alpha') = e^{jkds'sin\theta cos(\phi-\alpha'+\frac{\beta'}{2})} \quad (11)$$

A convolution form in the variable $\alpha'$ can be recognized for the inner integral appearing in (8), so leading to apply the Fourier transform for its computation, by invoking the convolution theorem as [8]:

$$T(\theta,\phi) = \int_0^{\frac{\rho_{max}}{d}} \mathcal{F}^{-1} \left\{ \widetilde{q}_1(s',w) \cdot \widetilde{r}(\theta,\phi,s',w) \right\} ds' \quad (12)$$

where:

$$\widetilde{q}_1(s',w) = \mathcal{F}\left\{ q_1(s',\alpha) \right\} \quad (13)$$

$$\widetilde{r}(\theta,\phi,s',w) = \mathcal{F}\left\{ r(\theta,\phi,s',\alpha') \right\} \quad (14)$$

and the symbols $\mathcal{F}$ and $\widetilde{\ }$ are used to denote the Fourier transform operator.

Let us consider a near-field spiral trajectory with samples locations at coordinates:

$$\alpha_m = m\Delta\alpha, \qquad m = 0, 1, 2, ..., M-1 \quad (15)$$

$$s_{nm} = \frac{\rho_{nm}}{d}, \qquad n = 0, 1, 2, ..., N-1 \quad (16)$$

where:

$$\rho_{nm} = a(\alpha_m + 2\pi n) \quad (17)$$

$N$ being the number of loops in the spiral arrangement and $M$ the number of samples for each loop.

After inserting relation (17) into equation (16) and making use of expressions (5) and (6), a pair of discrete mathematical relationships

are obtained which uniquely describe the near-field spiral trajectory in terms of spacings coherent with the plane-polar sampling requirements, namely:

$$\Delta\alpha = \Delta\phi = \frac{\lambda}{2r_o} \tag{18}$$

$$\Delta s = \frac{\Delta\rho}{d} = \frac{\lambda}{2d} \tag{19}$$

where $r_o$ is the radius of the smallest sphere completely enclosing the AUT.

With the above assumptions on spiral samples distribution, the numerical computation of the radiation integral (12) can be performed as:

$$T(\theta,\phi) = \sum_{n=0}^{N-1}\sum_{m'=0}^{M-1}[\widetilde{q}_1(s_{nm},w)\cdot\widetilde{r}(\theta,\phi,s_{nm},w)]\cdot e^{j\frac{2\pi m' w}{M}} \tag{20}$$

In this latter relation, the terms:

$$\widetilde{q}_1(s_{nm},w) = \frac{1}{M}\sum_{m=0}^{M-1} q_1(s_{nm},\alpha_m)\cdot e^{-j\frac{2\pi m w}{M}} \tag{21}$$

$$\widetilde{r}(\theta,\phi,s_{nm},w) = \frac{1}{M}\sum_{m=0}^{M-1} r(\theta,\phi,s_{nm},\alpha_m)\cdot e^{-j\frac{2\pi m w}{M}} \tag{22}$$

represents the Discrete Fourier Transform (DFT) of the sequences $q_1(...)$ and $r(...)$, respectively, which can be efficiently performed by adopting the FFT algorithm [8].

An overview of the data processing method for far-field computation from near-field samples on planar spiral is reported under Fig. 3.

## 4. NUMERICAL RESULTS

Numerical tests on dipole arrays are performed to show the effectiveness of the proposed far-field transformation process from near-field samples on planar spiral. As a first case, a circular array of 18 y-oriented Huyghens sources $\lambda/2$ spaced is considered, with excitation coefficients chosen to have a main lobe in the direction $\theta = 10°$ in the $H$-plane. Near-field acquisition is simulated on a plane at a distance $d = 10\lambda$ from the array, with samples lying on a planar spiral having $N = 20$ loops and M=136 points along each loop. Sampling spacings

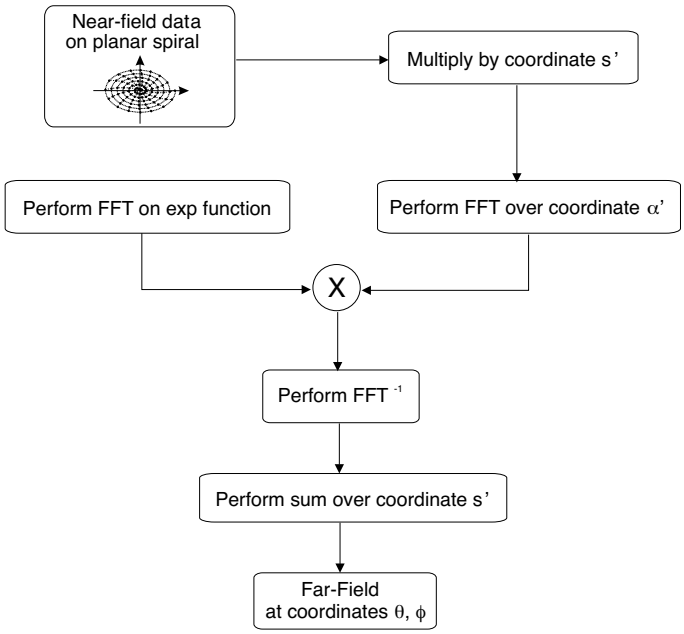


**Figure 3.** Data processing scheme for the planar spiral configuration.

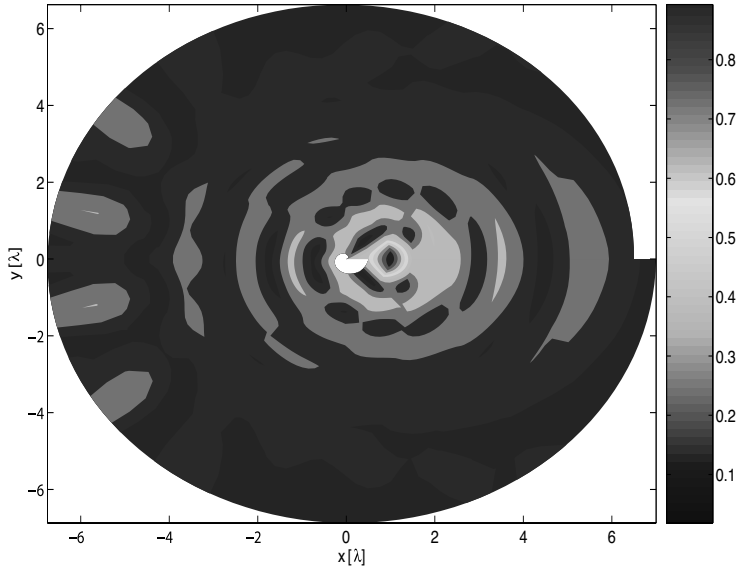


**Figure 4.** Normalized near-field amplitude on planar spiral for a circular array of 18 elements.

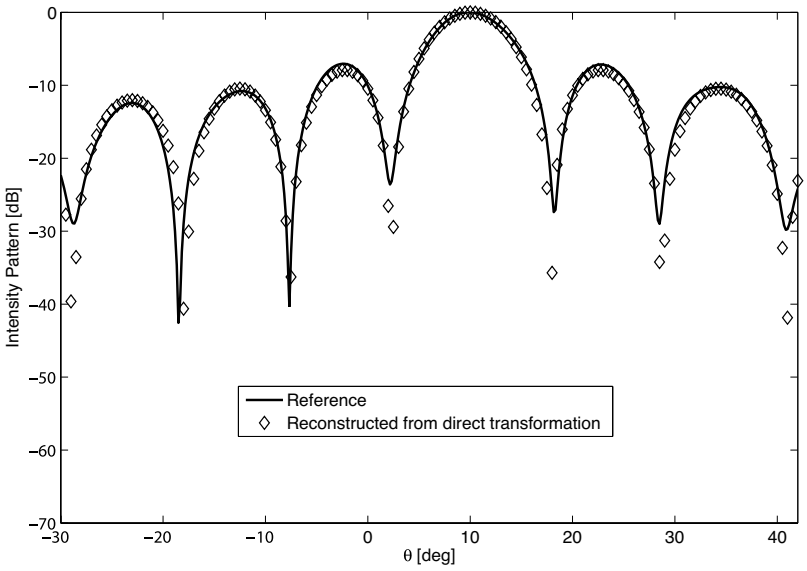


**Figure 5.** Co-polarized $H$-plane pattern for circular array of 18 elements.

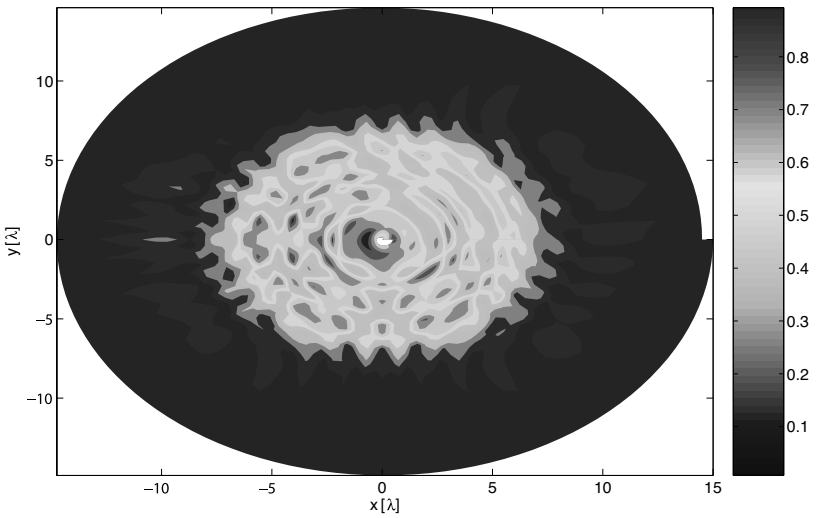


**Figure 6.** Normalized near-field amplitude on planar spiral for a planar circular array.

$\Delta\alpha$ and $\Delta s$ coherent with relations (18) and (19) are considered, by assuming $r_o = 10.85\lambda$. The contour plot of the normalized intensity pattern on the near-field spiral trajectory is shown in Fig. 4. The direct transformation algorithm is then applied to near-field spiral samples for recovering the co-polarized $H$-plane pattern reported under Fig. 5 and successfully compared with the exact array solution. As a further validation, a planar circular array of diameter equal to $14\lambda$ is considered, with elements given by $y$-oriented dipoles radially and azimuthally spaced of $\lambda/2$. Simulations are performed on a near-field plane at a distance $d = 15\lambda$ from the array, with samples located on a spiral arrangement with $N = 30$ loops and $M = 133$ points along each loop. An azimuthal spacing $\Delta\alpha = 2.72^\circ$ is assumed, with $r_o = 7.5\lambda$, and a normalized radial step $\Delta s$ as given by equation (19) is again considered. The normalized amplitude of the simulated near-field on the planar spiral is shown in Fig. 6, while the co-polarized $H$ plane pattern as obtained from the direct transformation algorithm is reported under Fig. 7. A high accuracy is proved again by comparison with the exact analytical solution.

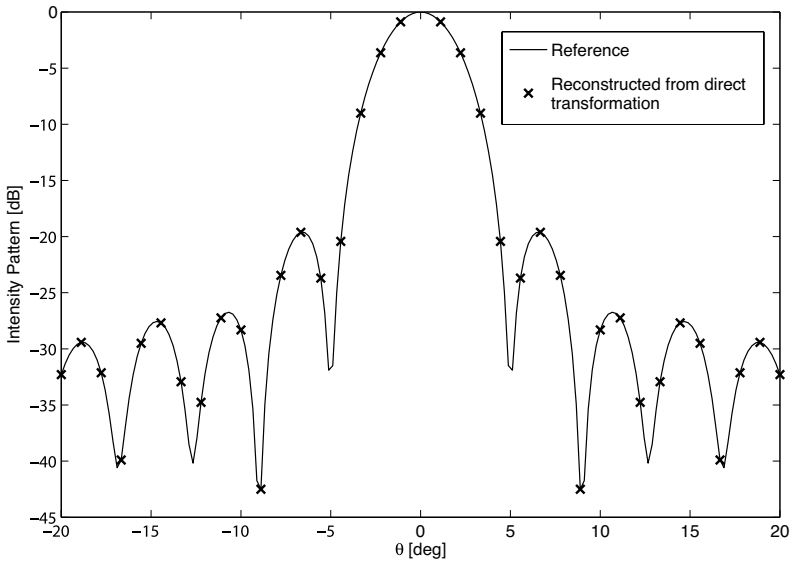


**Figure 7.** Co-polarized $H$-plane pattern for planar circular array.

## 5. CONCLUSIONS AND FUTURE DEVELOPMENTS

A far-field transformation procedure directly performed on near-field samples coming from a planar spiral arrangement is developed in this paper. The convolution property of the radiation integral is exploited to efficiently perform its computation in terms of FFT. This avoids the use of interpolation techniques usually adopted in literature to obtain a rectangularly regularized format of the near-field data which enables the application of the well known planar near-field to far-field transformation. The proposed data processing is numerically validated on circular arrays of elementary dipoles. Concerning future developments, two open points will be considered. First of all, the procedure will be extended to take into account the directive effect of a non-ideal probe, by including a correct probe compensation. Furthermore, the application of a two-probes based method [9] will be considered for recovering the far-field pattern from the knowledge of intensity-only data on a single near-field spiral surface.

## REFERENCES

1. Ayestaran, R. G. and F. Las-Heras, "Near field to far field transformation using neural networks and source reconstruction," *Journal of Electromagnetic Waves and Applications*, Vol. 20, No. 15, 2201–2213, 2006.
2. Williams, L. I., Y. Rahmat-Samii, and R. G. Yaccarino, "The bi-polar planar near-field measurement technique, Part I: Implementation and measurement comparison," *IEEE Trans. Antennas Propag.*, Vol. 42, No. 2, 184–195, 1994.
3. Yaccarino, R. G., L., I. Williams, and Y. Rahmat-Samii, "Linear spiral sampling for the bipolar planar near-field antenna measurement technique," *IEEE Trans. Antennas Propag.*, Vol. 44, No. 7, 1049–1051, 1996.
4. Bucci, O. M., C. Gennarelli, and C. Savarese, "Fast and accurate near-field far-field transformation by sampling interpolation of plane-polar measurements," *IEEE Trans. Antennas Propag.*, Vol. 39, No. 1, 48–55, 1991.
5. D'Agostino F., C. Gennarelli, and G. Riccio, "Theoretical foundations of near-field far-field transformations with spiral scannings," *Progress In Electromagnetics Research*, PIER 61, 193–214, 2006.
6. D'Agostino, F., F. Ferrara, C. Gennarelli, and G. Riccio, "Directivity computation by spherical spiral scanning in near-

field region," *Journal of Electromagnetic Waves and Applications*, Vol. 19, No. 10, 1343–1358, 2005.

7. Costanzo, S. and G. Di Massa, "Direct far-field computation from bi-polar near-field samples," *Journal of Electromagnetic Waves and Applications*, Vol. 20, No. 9, 1137–1148, 2006.
8. Weaver, H. J., *Theory of Discrete and Continuous Fourier Analysis*, John Wiley and Sons, New York, 1989.
9. Costanzo, S. and G. Di Massa, "Far-field reconstruction from phaseless near-field data on a cylindrical helix," *Journal of Electromagnetic Waves and Applications*, Vol. 18, No. 8, 1057–1071, 2004.